An observational study of ecohydrology of a sparse grassland at the edge of the Eurasian cryosphere in Mongolia

Yinsheng Zhang
Institute of Observational Research for Global Change, Yokosuka, Japan

E. Munkhtsetseg[1]
Institute of Meteorology and Hydrology, Ulan Bator, Mongolia

T. Kadota and T. Ohata
Institute of Observational Research for Global Change, Yokosuka, Japan

Received 29 September 2004; revised 29 March 2005; accepted 1 April 2005; published 20 July 2005.

[1] Between July 2002 and June 2004 we recorded many ecohydrological observations at a sparse grassland site on the southern periphery of the Eurasian cryosphere in Mongolia. Grass growth at the study site shows significant difference of biomass between drier and moister years. Seasonal change of PAR albedo is a good indicator of temporal change of biomass. The stresses of atmosphere and soil water to grass have been evaluated at the study site using index of air temperature stress degree-day (SDD) and soil water stress (SWS). SDD was small and prevailingly negative. Variations in the SWS tracked precipitation fluctuations. Variability of two indexes may imply that atmospheric heat stress for the growing grass was weak compared to soil water stress for such a semiarid region. The above conclusion is supported by irrigation experimental observation as well; clear differences of biomass were observed between watered and unwatered ground after irrigation commenced. Soil evaporation and transpiration were estimated using a soil moisture parameterization and verified with micro-Lysimeter observations. Variability of evapotranspiration shows temporal decline processes' response to precipitation events or snow melting. During the observation period, evapotranspiration totaled 301.6 mm, and precipitation totaled 319.5 mm. The mean partition of transpiration in evapotranspiration was 22%, which was small during wetter grass-growing periods but large in drier periods. The growing period is short along the periphery of the cryosphere, but water fluxes during the growing period contribute significantly to the annual water cycle.

Citation: Zhang, Y., E. Munkhtsetseg, T. Kadota, and T. Ohata (2005), An observational study of ecohydrology of a sparse grassland at the edge of the Eurasian cryosphere in Mongolia, *J. Geophys. Res.*, *110*, D14103, doi:10.1029/2004JD005474.

1. Introduction

[2] The terrestrial biosphere has an important influence on climate through the active regulation of water and energy fluxes. Processes within the terrestrial biosphere and atmosphere are intrinsically coupled with the hydrologic cycle. The coupling mechanism in the biosphere-atmosphere system is nonlinear. In addition, it is bidirectional or multidirectional: Individual components of the system are both under the influence of, and impacting upon, the remaining parts of the system [*Hutjes et al.*, 1998]. Vegetation interacts with the atmosphere through several linked mechanisms. Vegetation actively controls the evaporation process through its internal physiology. Stomata open and close in response to environmental conditions affecting photosynthesis, including temperature, humidity, radiation, CO_2 concentration and soil moisture.

[3] Interactions between grassy land surfaces and the atmosphere can be summarized as follows: radiation absorption; evaporation from bare soil and water retained on the leaves; and transpiration and vertical diffusion of water through soil. The main task in considering these interactions is to account accurately for the role of vegetation. Past authors [*Sellers et al.*, 1986; *Dickinson*, 1987] have demonstrated that high-quality observations are needed to better define the ecohydrology of the ground surface.

[4] Mongolia is characterized by a long cold winter and a short warm summer [*Bereneva*, 1992]. Permafrost and seasonal frost rocks are present in northern Mongolia [*Tsegmid and Vorobiev*, 1990], along the periphery of the Arctic region. Grassland covers more than 80% of Mongolian territory. *Ma et al.* [2003] have clarified northeastern Mongolia to be a semiarid region with higher potential evaporation and lower wetness index. Vegetation cover development in such a

[1]Now at Arid Land Research Center, Tottori University, Tottori, Japan.

0148-0227/05/2004JD005474$09.00

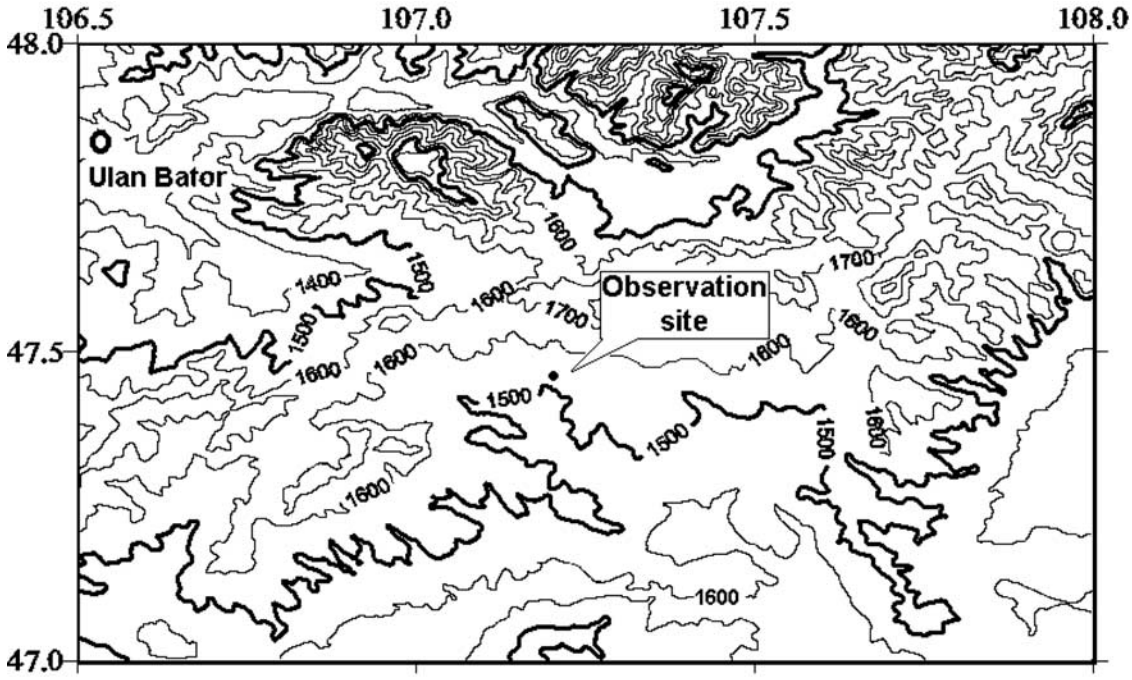

Figure 1. Location of the study site.

semiarid region strongly depends on the quantity plus the seasonal and geographical distribution of precipitation, e.g., clear relationship between grasses, and the precipitation and aridity index has been found in north China and southeast Mongolia [*Ni*, 2003]. *Miyazaki et al.* [2004] have documented that the precipitation and soil moisture before July had the most influence on grass growth in central Mongolia, and there is close relation of evapotranspiration and ground surface condition, know as LAI and soil moisture.

[5] The response of land surface processes to atmospheric forcing, and its feedback in Arctic and subarctic regions, is an important subject in the quest to better understand global and regional water cycles [*Vörösmarty et al.*, 2001], as well as ecohydrology [*Shaver et al.*, 2000]. As for the limits for the vegetation on a global scale, *Nemani et al.* [2003] presented significant growth stimulation in the northern high-altitude region and possible factor limiting the plant growth should be radiation regime. *Chapin* [2000] has demonstrated that hydrologic processes play a critical role in linking the land, atmosphere, and oceans of the Arctic System and in determining the role played by terrestrial ecosystems in feedbacks to climatic change. Relatively few works have considered the southern fringe of the Arctic region, such as Mongolia.

[6] This paper discusses results from a sparse grassland site along the southern periphery of the Eurasian cryosphere in Mongolia. Observations including heat/water fluxes and grassland phenology were recorded. The response of growing grass to climate and the hydrologic consequences of that growth were analyzed over a period of 2 years.

2. Observations

2.1. Site Descriptions

[7] An observation site was established on sparse grassland at Nalaikh in northeastern Mongolia at 47°45′N, 107°20′E, 40 km southeast of Ulan Bator. The site is on a sediment plain in a vast valley in the Tuul River basin (Figure 1); the nearest mountains, with relative heights of less than 500 m, are at least 10 km away. The topography at and around this site is very smooth.

[8] The observation site was in a semiarid region characterized by warm, dry summers [*Bereneva*, 1992]. Annual precipitation for the 2 years from July 2002 to June 2004 was 159.8 mm, 79% of which fell in the warm season (May to September). However, precipitation events were rarer in August than in July. The annual mean air temperature was −4.1°C, but air temperatures were an average of 12.7°C during the period of plant growth from May to September. The annual mean relative humidity was 61%. Specific humidity was 5.5 g/kg during the period of plant growth but 0.5 g/kg for other periods. The prevailing wind was from the NW-ENE with annual mean wind speed of 2.6 m/s. The wind was stronger (mean wind speed of 3.2 m/s) during the period of plant growth.

[9] The annual mean global solar radiation flux was 168.5 Wm^{-2}. The average albedo was 0.71 during periods of snow cover, and 0.12 for periods without snow. Accordingly, the average net radiation was −6.0 Wm^{-2} and 60.0 Wm^{-2} respectively.

[10] Mongolian soil generally includes a broad distribution of detrital rock sediments that influence soil formation. Common soils are light loams and loamy sand, mainly not salinized, with considerable amounts of rock detritus and pebbles [*Nogina*, 1978, 1989]. The soil in the study region was sandy, with little organic matter, and less than 10 cm in thickness. Large sand grains occurred beneath the organic layer. Figure 2 shows the vertical profiles of soil porosity and bulk density at the study site; the former decreased with depth, while the latter increased. Soil field water capacity and wilting point were also determined in the surface layer (0–50 cm

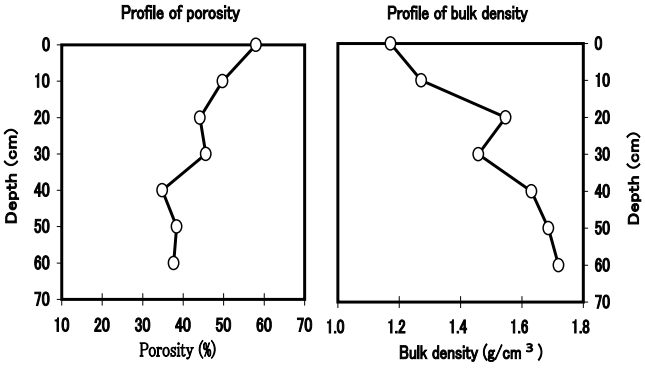

Figure 2. Profiles of soil porosity and bulk density to 60 cm depth at the study site.

depth) at the study site. The former was measured in the field and the latter was determined in the laboratory. Soil water capacity ranged from 6.5–17.2% and wilting point ranged from 2.8–4.1% in the surface layer.

[11] The observation site was on the periphery of the subarctic permafrost region [*Sharkhuu*, 2001]. A thick active layer and higher ground temperatures characterize permafrost regions. Figure 3 shows the ground temperature profiles to 30 m depth at the study site, measured by borehole on two occasions (9 November 2002 and 15 July 2003). The downward and upward frost front was at 2 m and 5 m respectively on 9 November 2002, and the downward thaw front was at 5 m on 15 July 2003. At depths exceeding 7 m, ground temperature varied slightly around 0°C, which is characteristic of permafrost on the periphery of a discontinuous permafrost region with high ground temperature. This has been classified as warm permafrost [*Ishikawa et al.*, 2005].

[12] Observations of ground temperature from the surface down to 3 m show that the surface temperature was continuously below 0°C at the beginning of October. The downward frost front moved from the surface to 3 m in 85–90 days. After the snow cover disappeared at the beginning of April, the surface started melting. The downward moving thawing front reached 3 m at the end of April. Seasonality of the permafrost active layer suggests that the thaw-frost cycle may not affect grass biological processes because the thaw depth exceeded 3 m during its growth period (May to September), even though the study site was underlain by permafrost.

[13] Vegetation was uniformly sparse grass with a coverage of 38–60% during the maximum growth period. Over the pasture, plant type and species did not vary. Artemisia frigita dominated (~60%) and other species included Arenaria and Leymus chinensis. The maximum grass height in mid-July was less than 20 cm. Figure 4 shows the vertical distribution of grass root density (dry biomass) measured in April and June 2003. Grass roots develop mainly in the surface ground layer (the top 50 cm). Differences in root biomass between April and June also occurred only in the ground surface layer. Figure 4 suggests that the root zone at the study site was the layer between the soil surface and 50 cm depth.

2.2. Observations

[14] An observation site was established on 1 July 2002 on grassland at Nalaikh, southeast of Ulan Bator. An automatic climate observation system (ACOS) recorded air temperature, humidity and wind speed at heights of 0.5, 1.0, 2.0 and 4.0 m. Short-wave radiation, long-wave radiation and photosynthetically active radiation (PAR) were measured in both upward and downward directions. In addition, sensors measuring air pressure and an infrared radiative thermometer recording grass leaf temperature and net radiation were installed 1.5 m above the ground surface. Detailed information on instruments used in this work is summarized in Table 1.

[15] The measured precipitation from gauge has long been known to underestimate true precipitation amounts. *Zhang et al.* [2004] estimated the bias of the gauge-measured annual precipitation to be 17 to 42% in Mongolia. *Yokoyama et al.* [2003] discussed in detail the bias of the

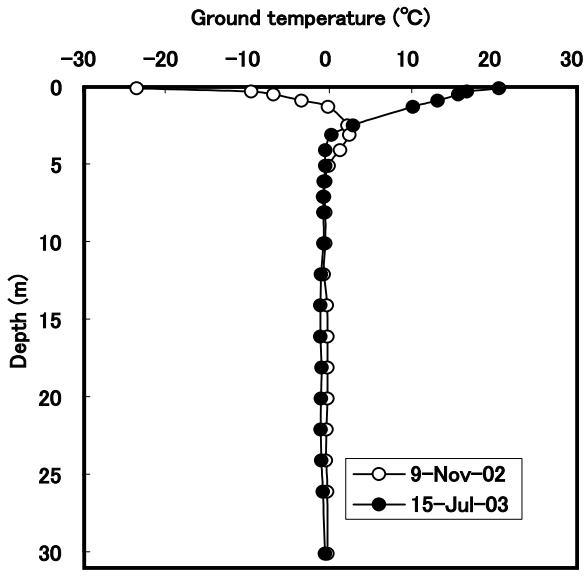

Figure 3. Ground temperature profiles to 30 m depth at the study site on 9 November 2002 and 15 July 2003.

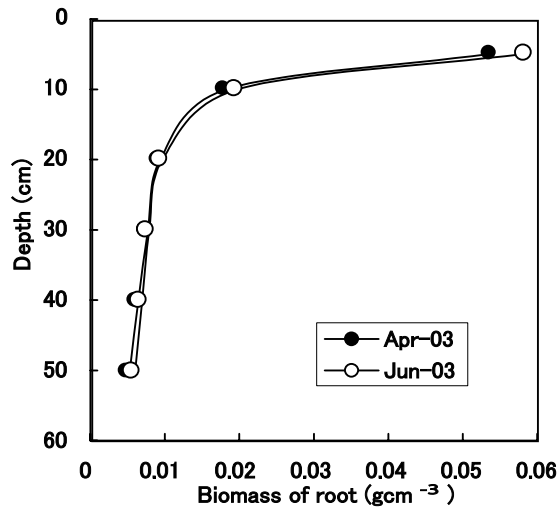

Figure 4. Vertical profile of grass root biomass at the observation site in April and June 2003.

Table 1. List of Instruments Used in This Work

Item	Units	Instrument (Model, Manufacturer)	Recording Interval
Short-wave radiation	Wm^{-2}	radiometer (MS402, EKO, Japan)	10 min
Long-wave radiation	Wm^{-2}	infrared radiometer (MS202, EKO, Japan)	10 min
All-wave net radiation	Wm^{-2}	net radiometer (REBS Q7, REBS, Inc., United States)	10 min
Photosynthetically active radiation	$\mu Es^{-1}\ m^{-2}$	optical photon-meter (PAR-01, REBS, Inc., United States)	10 min
Wind speed	m/s	anemometer (AC750, Kaijo Corporation, Japan)	10 min
Wind direction	deg	anemometer (VR036, Kaijo Corporation, Japan)	10 min
Snow depth	cm	ultrasonic level-meter (SR50, Kaijo Corporation, Japan)	60 min
Precipitation	mm	Tipping bucket rain gauge (52202, R. M. Young Com., United States)	10 min
Air temperature	°C	humidity and temperature probe (HMD45D, Vaisala Oyj, Finland) with ventilation pipe (PVC-02, PREDE, Japan)	10 min
Relative humidity	%	humidity and temperature probe (HMD45D, Vaisala Oyj, Finland) with ventilation pipe (PVC-02, PREDE, Japan)	10 min
Surface temperature	°C	infrared radiation thermometer (CML303F, CLIM., Inc., Japan)	10 min
Heat flux in the soil	Wm^{-2}	heat flux plate (PHF01, REBS, Inc., United States)	10 min
Volumetric water content	m^3/m^3	ECHO probe (EC-10, Decagon Devices, Inc., United States)	10 min
Soil temperature	°C	Pt-thermometer (TPT100S, CLIMATEC, Inc., Japan)	10 min
Air pressure	hPa	analog barometer (PTB101B, Vaisala Oyj, Finland)	10 min

gauge used in this work; the precipitation data of our observation have been corrected using their procedure, which implies a bias of 17%.

[16] Soil moisture was observed automatically and manually. Seven time domain reflectometry (TDR) probes and seven Pt thermometers were installed at depths of 0, 0.2, 0.4, 0.8, 1.2, 2.4 and 3.0 m; also, two sets of heat flux meters were set at 0.02 and 0.2 m. Along with a data logger, these sensors comprised the soil monitoring system (SMS). Soil moisture in the surface layer (0–60 cm) was also manually sampled to calibrate TDR data.

[17] Phenology observations included the coverage and biomass of grass and water content in grass leaves and were made at 10 day intervals from July 2002 to June 2004. Observations were conducted at four 50 × 50 cm plots; the presented results are averages from these four plots.

[18] Evapotranspiration and soil and potential evaporation rates were observed using microlysimeters. Lysimeters were installed by setting a cylindrical container into the soil level with the natural surface. The cylinder enclosed a block of natural soil. Weight changes were measured each day, and evaporation was evaluated with the following equation [*Allen*, 1990]:

$$Ely = \Delta W/S + Pr \tag{1}$$

where Ely is evaporation measured by Lysimeter method, ΔW is the weight difference of the Lysimeter, S is the surface area of the soil within it, and Pr is precipitation. The soil in the drum was changed every day and was carefully selected to ensure that its layer-by-layer constitution matched as closely as possible that of nearby, undisturbed soil, and that placement relative to the natural surface was maintained.

[19] Grass phenological comparisons were carried out in an 8 × 8 m study area to investigate the response of grass growth to available moisture. Half of the study area received 2 mm water per day. A microlysimeter was set in the watered area to quantify changes in evapotranspiration rates during irrigation.

2.3. Calculation Method

[20] Sensible and latent heat fluxes during the snow-free period were calculated using the heat budget method:

$$Qn = Qh + Qe + Qg \tag{2}$$

$$Qe = \frac{Qn - Qg}{(1+\beta)} \text{ and } Qh = \frac{Qe}{\beta} \tag{3}$$

$$\beta = \frac{C_P}{L_e}\frac{(T_2 - T_1)(U_2 - U_1)}{(q_2 - q_1)(U_2 - U_1)} \tag{4}$$

Here, Qn is the net radiation, Qh is the sensible energy, Qe is the latent energy, Qg is the ground energy flux, β is the Bowen ratio, C_P is the specific energy at a constant pressure, Le is the latent energy of vaporization, U is the wind speed, T is the air temperature, q is the specific humidity, and the subscripts 2 and 1 denote different heights. It is necessary to mention that molecular diffusivities for heat and water were assumed to be close sufficiently. In nighttime, such assumption is usually broken. Therefore evaluating Qh and Qe using equation (3) requires accurate measurements for all variables with time interval less than 30 min [*Oke*, 1987].

[21] Potential evaporation (Ep) is calculated by the Penman method [*Brutsaert*, 1982]:

$$Ep = \frac{\Delta}{\Delta + \gamma} Qne + \frac{\gamma}{\Delta + \gamma} Ea \tag{5}$$

where Δ is the slope of the saturation water vapor pressure curve, and γ is

$$\gamma = C_P P/0.622 L_e \tag{6}$$

where P is air pressure. Qne is the heat energy available for evaporation, as determined by the net radiation (Qn) and ground heat flux (Qg):

$$Qne = (Qn - Qg)/L_e \tag{7}$$

Ea is, drying power of air, a function of wind speed (U) and the saturation deficit ($e_0 - e$):

$$Ea = 0.26(1 + 0.45U)(e_0 - e) \tag{8}$$

[22] Soil evaporation and transpiration are partitioned. Evaporation from soil water, *Esoil*, was estimated with the α-parameterization method:

$$Esoil = \frac{\rho}{Ra}[\alpha q_{SAT}(Ta) - q_A] \tag{9}$$

where ρ is air density; $q_{SAT}(Ta)$ is the saturated specific humidity at the surface temperature *Ts*, q_A is air specific humidity, and *Ra* is an aerodynamic resistance that can be calculated by profiles of air temperature, humidity and wind speed. The coefficient α is parameterized [*Noilhan and Planton*, 1989]:

$$\alpha = \begin{cases} 1 & \theta \geq \theta_{FC} \\ \frac{1}{2}\left[1 - \cos\left(\frac{\theta}{\theta_{FC}}\frac{\pi}{2}\right)\right] & \theta < \theta_{FC} \end{cases} \tag{10}$$

where θ and θ_{FC} is surface soil moisture and soil water capacity respectively. Therefore transpiration E_{TRANS} from grass was estimated by $E = E_{SOIL} + E_{TRANS}$, E is evapotranspiration which can gained from latent heat *Qe*.

3. Results and Analysis

3.1. Grass Phenology and Its Correlation to Climate

[23] Plant phenology is an important variable in the study of terrestrial ecosystems and ecohydrology. For cold regions like the Arctic, several studies have documented alterations in plant growth associated with warmer temperatures due to global warming [*Myneni et al.*, 1997]. Phenological observations can demonstrate a consistent temperature-related shift or "fingerprint" and document the amount of change. Phenological studies have recently been used to analyze climatic and ecological changes and have prompted substantial new scientific interest in seasonal-to-decadal-scale vegetation dynamics [e.g., *Schwartz*, 1999; *Lucht et al.*, 2002].

[24] Field observations of species-level phenophases have been linked to local and regional climatic variations occurring over several decades [*Beaubien and Freeland*, 2000; *Chmielewski and Rotzer*, 2001]. Figure 5 shows the observed phenological results at our study site from July 2002 to June 2004, including the parameters of coverage, biomass and water content of grass leaves, and the associated 10 day values for climatic elements. Significant differences in grass phenology occur later in every growing period but not earlier. The maximum grass coverage in 2003 was 55.7%, 10.7% higher than the maximum coverage in 2002. Similarly, the maximum biomass and water content in grass was 114.4 gm^{-2} and 66.3% in 2003, versus 61.9 gm^{-2} and 68% in 2002.

[25] Corresponding differences in climatic conditions occurred in precipitation and air temperature but not in global solar radiation. Precipitation totaled 27.8 mm from July to August of 2002 and 81.1 mm from July to August of 2003. Air temperature was 18.8°C in 2002, and 14.4°C in 2003; mean global solar radiation flux was 226.8 Wm^{-2} in 2002 and 228.0 Wm^{-2} in 2003. Grass growth in the study region was restricted by heat conditions but well correlated with water supplies.

3.2. Growth Period Estimation

[26] Visual observations and seasonal patterns of green biomass determine grass activity periods [e.g., *Kim and Verma*, 1996; *Burba et al.*, 1999]. These determinations are however limited because of inaccuracies in biomass determination when values are small and difficulties in determining emergence dates at remote sites that are infrequently sampled. Furthermore, many recent investigations have recognized that actual grass activity is determined physiologically (via grass responses to environmental conditions at a given stage of plant development) and would not necessarily be described by either foliage area or biomass alone [*Sakai et al.*, 1997; *Lingakumar and Kulandaivelu*, 1998]. Such problems can be mitigated through the use of an easily measurable radiative property of the grass (e.g., photosynthetically active radiation albedo (PAR albedo, α_{PAR}), short-wave radiation albedo, absorbed photosynthetically active radiation, far and near-infrared reflectance, greenness) that would simplify interpretation of biomass data. This study uses α_{PAR} in conjunction with biomass data to improve estimates of vegetation growth.

[27] Growth periods between July 2002 and June 2004, determined from daily averaged measurements of α_{PAR} in conjunction with biomass estimates, are shown in Figure 6. Activity was divided into ten major periods of five types: pregrowth, early growth, peak growth, senescence and postsenescence. Postsenescence included snow covered periods at the study site. In a drier summer of 2002, in spite of an increase in α_{PAR} from 1 July to mid-August, which suggests a weakening of grass photosynthesis, biomass varied stably around 40 gm^{-2} during the peak growth period. Afterward, grass senescence began as reflected in the increase in α_{PAR} until the beginning of October, at which time the ground froze and later became snow covered until late March. These periods were classified as senescence and postsenescence (or snow covered). As the snow melted (1 April 2003 to 1 May 2003), the ground thawed but no biological activity occurred because of the low temperatures. This was the pregrowth period. From early May to late June 2003, a moister year, α_{PAR} gradually decreased as grass biomass increased, but biomass was less than 40 gm^{-2}, suggesting early growths in grass activity. During early growth, the green component of vegetation became noticeable against the yellow soil color, as α_{PAR} albedo decreased from 11 to 7%. Peak growth occurred between 1 July and 31 August 2003. The figure shows that peak growth is characterized by maximum values in biomass and minimum values in α_{PAR}. Subsequently, α_{PAR} again increased, indicating senescence. The following year, the growing period repeated but with date differences forced by air temperature variations. Section 3.7 examines growth periods (determined using both approaches) in terms of the seasonal distributions of energy and water fluxes between the atmosphere and the surface.

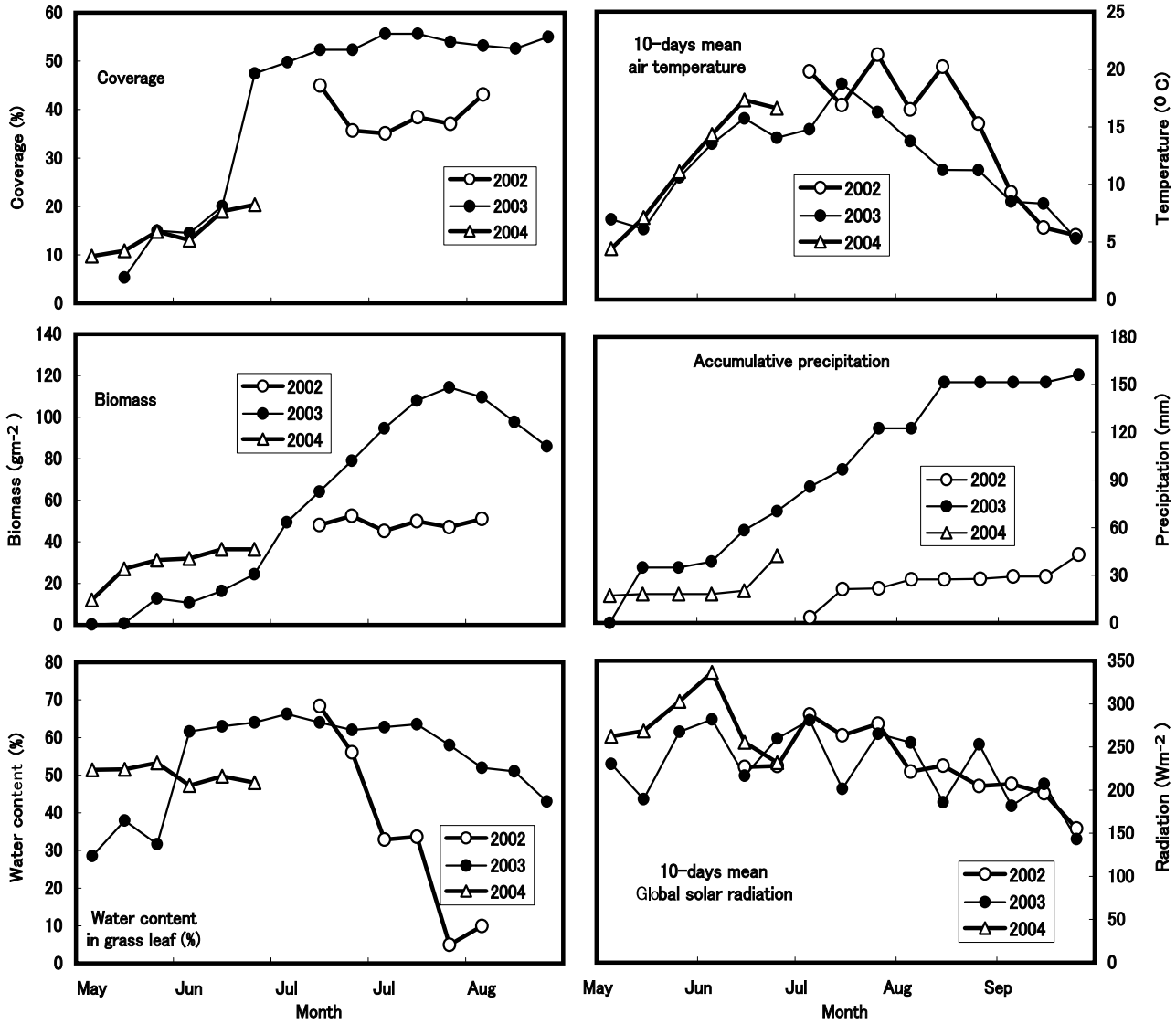

Figure 5. Phenological results at the study site from July 2002 to June 2004, with 10-day response values for climatic elements.

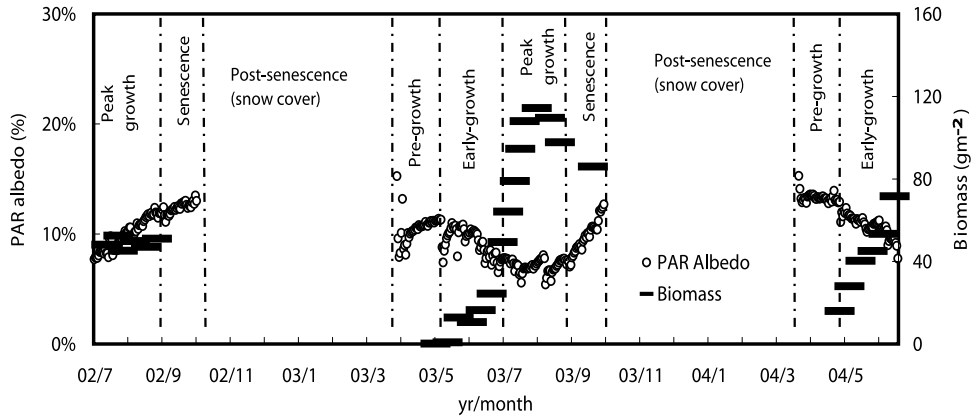

Figure 6. Determination of growth periods between July 2002 and June 2004 from daily average PAR albedo (α_{PAR}) in conjunction with biomass observations.

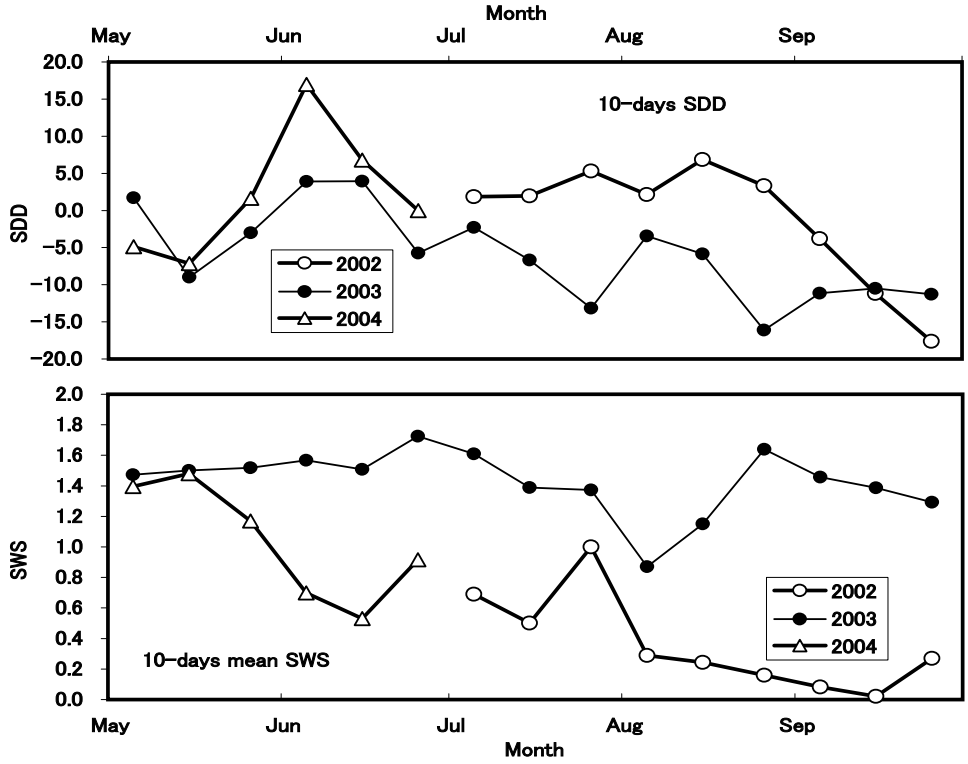

Figure 7. Ten-day values of air temperature stress degree days (SDD) and 10-day mean soil water stress (SWS) between July 2002 and June 2004 at the study site.

3.3. Atmosphere Heat Stress and Soil Water Stress on Grass

[28] The use of temperature as an indicator of plant growth has been studied in detail over the past 30 years [*Jackson*, 1982; *Idso*, 1982]. Several researchers have demonstrated the use of grass temperature in water stress detection and quantification [*Jackson et al.*, 1977; *Kirkham et al.*, 1983; *Sivakumar*, 1986]. *Walker and Hatfield* [1979] demonstrated that the growth stage depends on grass temperature. They showed that pasture yield was strongly related to stress degree days (SDD). SDD sums differences in grass temperature above ambient air temperature for the growth phase of interest [*Jackson et al.*, 1977]. *Idso et al.* [1977] define the SDD index as

$$SDD = \sum_{i}^{n} (Ts - Ta) \tag{11}$$

where $Ts - Ta$ is the grass-air temperature difference and n is the number of measurement days during the period of interest. Ts was measured by infrared thermometers in this study.

[29] Water stress in plants depends on evaporative demands of the atmosphere and soil water availability. Evaporative demands are represented by vapor pressure deficits; the extent to which evaporative demands can be met depends on soil water and relative leaf area. Plant temperature and water stress are related: If soil moisture is limited, stomata close. Reduced transpirational cooling allows grass temperatures to increase to values warmer than those of the air [*Pearcy et al.*, 1971].

[30] In several model approaches, a soil water stress (SWS) function that depends on soil water content is applied. For example, *Noilhan and Planton* [1989] define the extractable soil water content as

$$SWS = \frac{\theta - \theta_{WILT}}{\theta_{FC} - \theta_{WILT}} \tag{12}$$

where θ is the soil volumetric moisture in the root zone, and θ_{FC} and θ_{WILT} are the root zone moisture content at field capacity and wilting point, respectively. In this study, the root zone was defined as 0 to 30 cm according to the root distribution (section 2.1). θ_{FC} and θ_{WILT} are 15.1% and 3.8%, respectively.

[31] Figure 7 shows both SDD and SWS at the study site in the growing season (May to September). SDD and SWS show contrary temporal variations. During the peak growth period of 2002 and the early growth period of 2004, SDD was large; SWS was consistently smaller. In contrast, in 2003, SDD was consistently negative during the entire growth period, whereas SWS consistently exceeded 1.4 except during mid-August. Precipitation for May to September of 2003 was 156.2 mm, and the mean air temperature was 11.7°C; as noted in section 2.1, the period was wet and cool.

3.4. Seasonal Variation of Evapotranspiration Coupling to Precipitation, Soil Moisture, and Potential Evaporation

[32] Evapotranspiration (E) was calculated using the heat budget method illustrated by equations (2)–(4), and is displayed in the second panel of Figure 8. Calculations were performed for 1 July to 2 October 2002; 1 April to 7 October 2003; and 26 March to 30 June 2004, i.e., the entire study period except for the postsenescence periods. Precip-

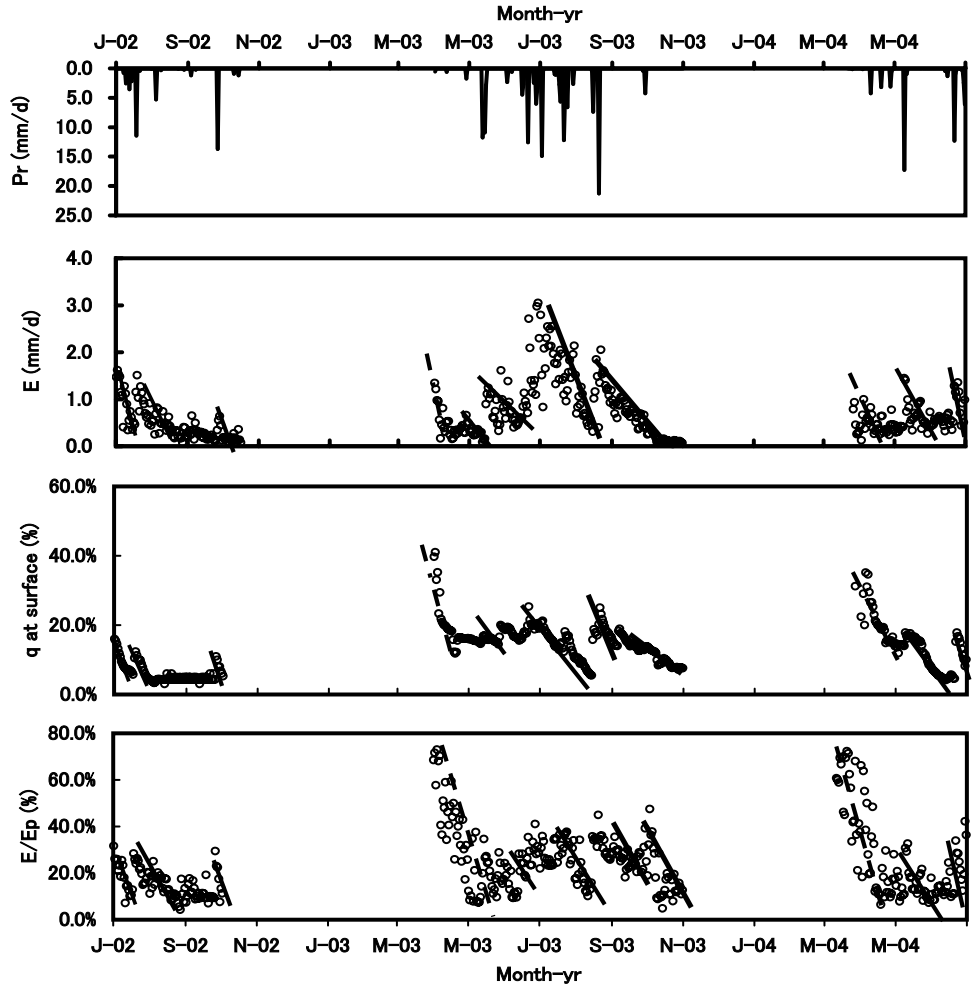

Figure 8. Seasonal variation of precipitation (*Pr*), calculated evapotranspiration (*E*), surface soil moisture (θ at surface), and evaporation coefficient (*E*/*Ep*) in the pregrowth and grass growth periods (early growth to senescence) between July 2002 and June 2004. The lines show declining processes of *E*, θ, and *E*/*Ep*. Black lines indicate precipitation processes; dashed lines reflect snowmelt processes.

itation (*Pr*) and surface soil moisture (θ at surface) are shown for the same periods in the top and third panels of Figure 8. The lines suggest the components are declining. Black lines show processes related to precipitation, while dashed lines shows processes related to snowmelt.

[33] The upper three panels in Figure 8 suggest that every declining process of *E* and θ at the surface can be initially linked to precipitation events (besides declines related to snowmelt, which occurred during pregrowth in 2003 and 2004). Differences in the sustained period of every declining process can be related to precipitation and soil water capacity, which both influence grass growth. Therefore, over semiarid sparse grassland, precipitation events or snowmelt can elucidate variations in peaks of evapotranspiration.

[34] From 1 July to 2 October 2002, before the ground surface froze, *E* totaled 48.9 mm and precipitation totaled 42.1 mm. *E* and *Pr* totaled 177.6 mm and 159.0 mm between 1 April and 7 October 2003 and 54.5 mm and 53.4 mm between 26 March and 30 June 2004. The ratio of *E*/*Pr* was 1.16, 1.12 and 1.02 for the three different years.

[35] Evapotranspiration that is theoretically limited by available energy can be expressed as potential evapotranspiration (*Ep*), which is a useful index to investigate ground surface conditions controlling evapotranspiration (*E*). If *Ep* is determined completely by atmospheric conditions, *E* normalized by *Ep* should depend only on the surface (soil/vegetation). However, most *Ep* concepts involve net radiation, which also relates *Ep* to surface conditions. *Ep* was calculated in this study using equations (5)–(8), and the normalized index *E*/*Ep*, the so-called evaporation coefficient, is shown in the lowest panel of Figure 8.

[36] Declines in *E*/*Ep* can be linked to temporal variations in surface θ, including those that occur after snowmelts. (In this period in April 2003 and 2004, surface soil moisture suddenly increased by more than 40%. The evaporation efficiency approached 0.8 and then decreased as soil moisture decreased.) *E*/*Ep* values indicate that ground surface conditions controlled evapotranspiration (*E*) efficiently in the study region.

[37] Some of the declining lines in Figure 8 are not exactly linear. Evapotranspiration at the study site was not determined solely by precipitation: It was also affected by

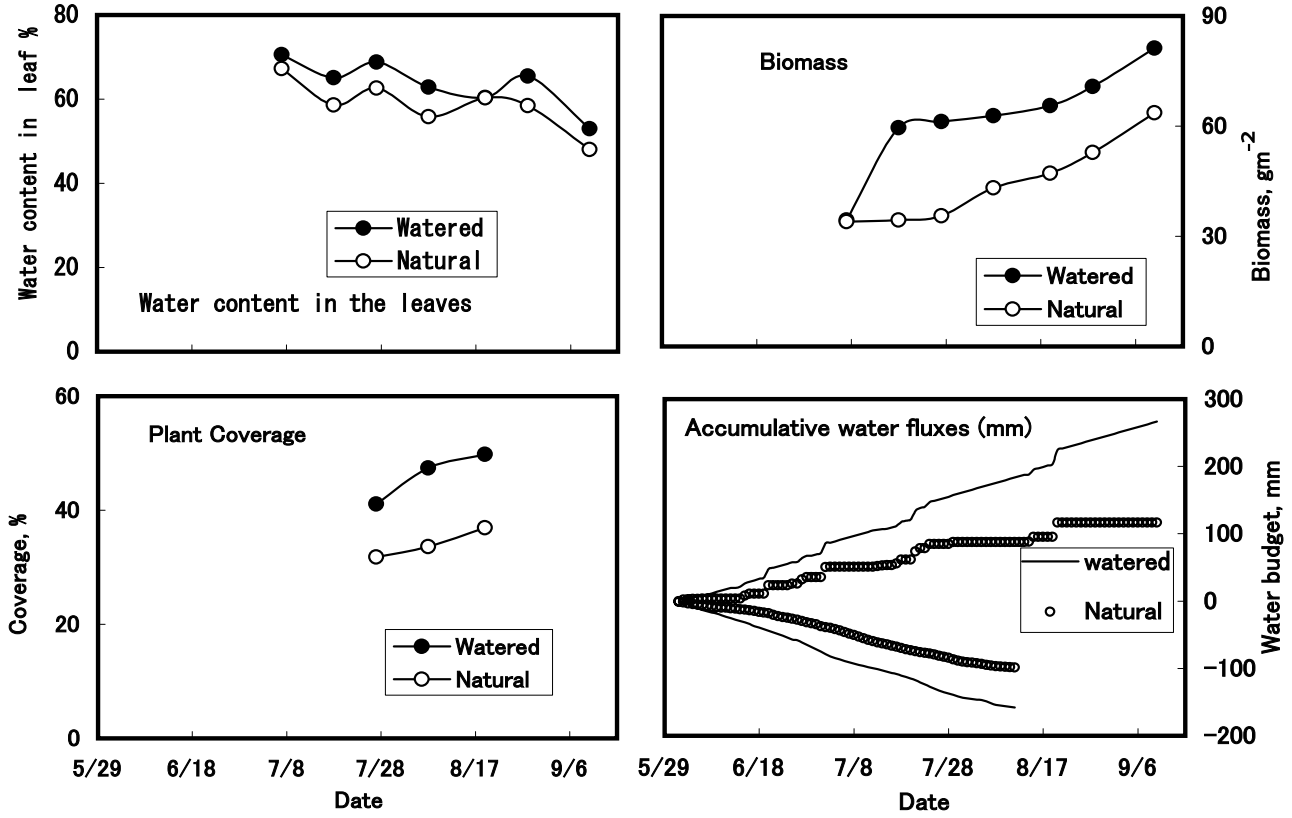

Figure 9. Comparison of grass phenology and water budget between a watered and a natural grassland between 1 June and 10 September 2003; the positive values in the lower right panel show received water at surface, and the negative values show evapotranspiration.

vegetation. For example, even when biomass is low, grass will still uptake water through its roots from the soil to supply transpiration.

3.5. Effect of Irrigation on Grass Growth and Evapotranspiration

[38] To investigate the effects of irrigation on grass growth and evapotranspiration, we regularly watered part of the study site up to 2.0 mm/day on days without precipitation from 1 June to 10 September 2003. The total precipitation in the period was 116.6 mm; therefore the received water on the watered field was 266.6 mm. Phenological observations were conducted on the field and also on unwatered ground nearby. A microlysimeter was also installed in the ground to address the effects of irrigation on evapotranspiration. Figure 9 shows the comparison between the watered and unwatered (natural) study areas.

[39] No significant differences in phenological components were observed between watered and unwatered areas until 7 July, that is, after 36 days of watering. A large difference in biomass (25.2 gm^{-2}) was recorded on 18 July. Water content in unwatered grass leaves decreased, with higher values observed in leaves in the watered field. In contrast, a clear difference in evapotranspiration was observed between the two areas. From 1 June to 11 August, total evapotranspiration was 158.0 mm in the watered field and 98.8 mm in the natural field. Between 1 June and 7 July, total evapotranspiration in the watered field exceeded that of the natural field by 42.6 mm, even for areas with similar vegetation cover. Therefore differences in evapotranspiration between the two fields averaged 1.15 mm/day between 1 June and 7 July, but only 0.47 mm/day for other days. More than 75% of the irrigated water (2.0 mm/day) joined the water cycle in the subsurface layer and helped the grass to grow.

3.6. Partitioning Evapotranspiration Into Soil Evaporation and Transpiration

[40] The results described in section 3.2 suggested that evapotranspiration was determined not only by soil conditions but also by vegetation, although it may be sparse. Evapotranspiration (E) studies must confront two issues. One is the difficulty in separating E into its two components, soil evaporation (*Esoil*) and plant transpiration (*Etrans*). In addition, studies of E in regions characterized by partial or sparse plant canopy cover that account for a significant fraction of land surface are difficult because relative contributions to total E from soil and plant can vary throughout a day and a season.

[41] Because of limitations in climate and vegetation conditions, and the excessive time and personnel costs sometimes associated with field experiments, it is not practical to measure all parameters needed to verify and validate a simulation model. However, estimates of parameters obtained from a model can provide estimates of values that are difficult to measure. A mechanistic and calibrated model of E can be used to calculate daily and seasonal values of *Esoi*l and *Etrans* [*Lascano et al.*, 1994].

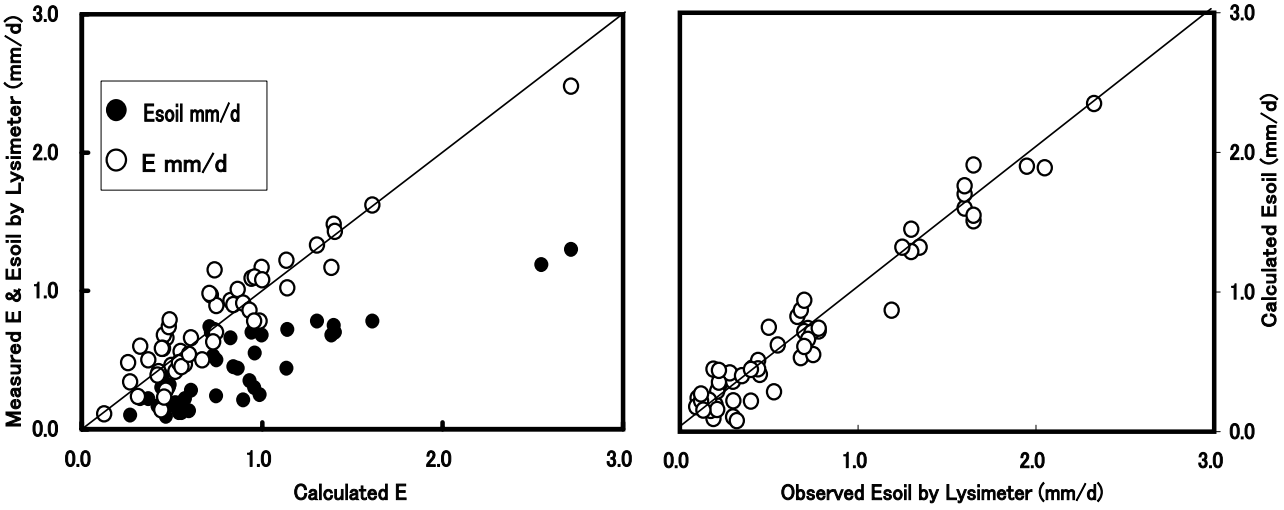

Figure 10. Comparisons of (left) observed evapotranspiration (*E*) and soil evaporation (*Esoil*) by microlysimeter methods versus calculated evapotranspiration rates (*E*) and (right) observed *Esoil* by microlysimeter methods versus calculated *Esoil* from equations (9) and (10).

[42] *Esoil* was calculated in this study using a parameterization introduced by *Noilhan and Planton* [1989] and summarized by equations (9) and (10). *Etrans* was estimated by the relationship $E = Esoil + Etrans$. The estimation results were verified from actual *E* and *Esoil* values recorded using microlysimeter methods.

[43] First, *E* and *Esoil* values obtained by microlysimeters were compared to *E* calculated by equations (2)–(4) in the left panel of Figure 10 to assess the veracity of the calculation. Observed and calculated *E* correlated well by coefficient of 0.9422 with significant level of 95% and standard error of 0.11 mm; observed *Esoil* was systemically smaller than *E* except on a few occasions just after snowmelt. In the right panel of Figure 10, *Esoil* values obtained by microlysimeter methods versus *Esoil* calculated by equations (9) and (10) are compared, the coefficient between them was 0.8632 with significant level of 95% and standard error of 0.09 mm. The results described in Figure 10 do not include values during the postsenescence period, when the ground was frozen or snow covered.

[44] Figure 11 shows 10 day partitions of values for *Esoil* and *Etrans*. There are clear seasonal variations. In the period 10–15 days after snowmelt, *Esoil* matched *E* perfectly. In this pregrowth period, grass stoma were not yet open. *Esoil* was close to *E* at the curve peaks because of precipitation events (see section 3.4).

[45] *Etrans* totaled 57.1 mm between July 2002 and June 2004, 20% of total *E*. Over the whole year of 2003, the annual *Etrans* was 15% of the annual *E*. *Etrans* was 30% of *E* in the latter half of 2002, and 38% of *E* in the early half of 2004. As noted in section 2.1, May to September 2003 was wetter than the other growing seasons observed during the study.

[46] *Esoil* is more sensitive to surface soil moisture than *Etrans*. The former takes water from a very thin soil layer and moves it to the atmosphere; the latter transfers water

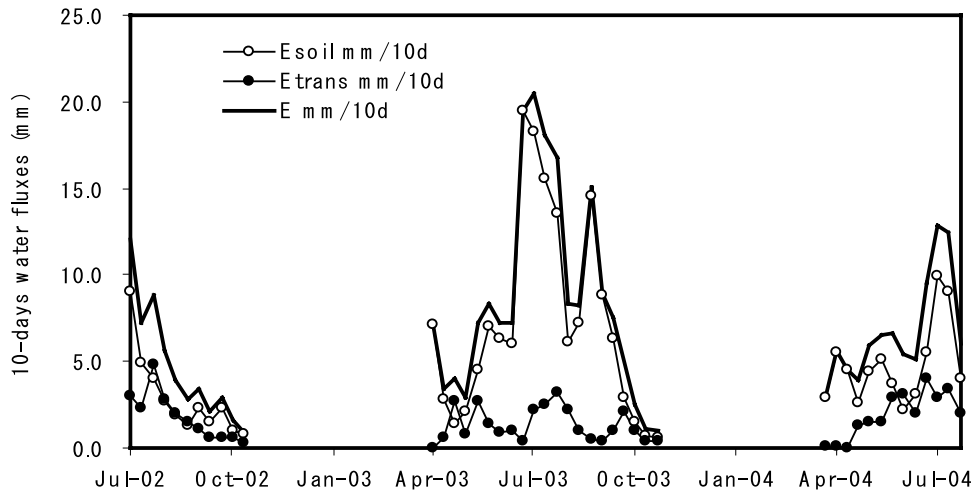

Figure 11. Seasonal variation of 10-day evapotranspiration (*E*), soil evaporation (*Esoil*), and transpiration (*Etrans*) rates at the study site from July 2002 to June 2004 (excluding postsenescence periods).

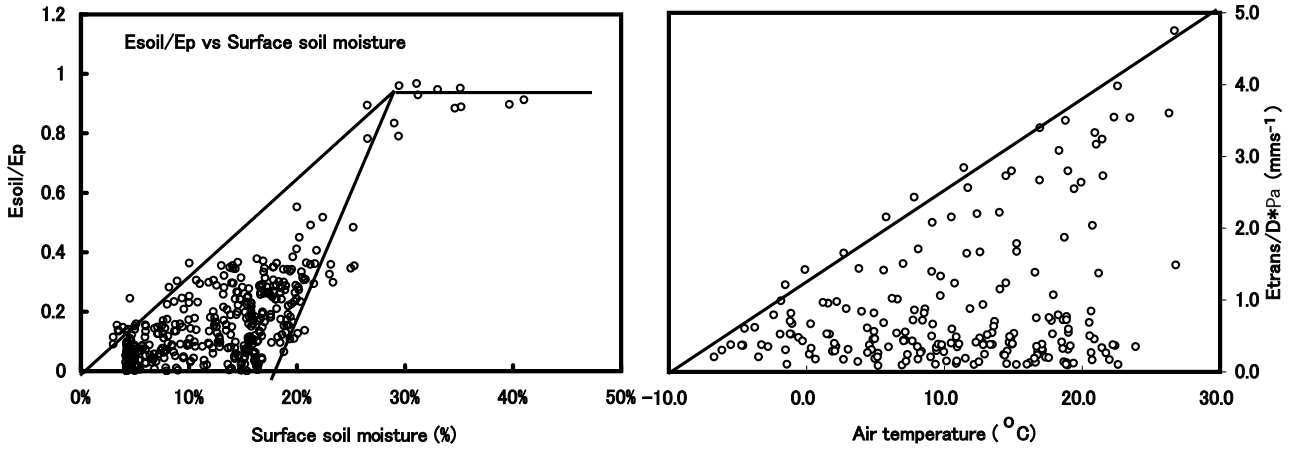

Figure 12. Relationships between (left) *Esoil*/*Ep* and surface moisture and (right) leaf conductance (*Etrans*/*D* * *Pa*, mms^{-2}) and air temperature. *D*, leaf-to-air specific deficit; *Pa*, air density.

from the soil through root-stalk-leaf mechanisms, and may take water from a thicker soil layer. Therefore *Etrans* is anticipated to be more independent of soil moisture variations than *Esoil*. Figure 12 (left panel) shows the variation in *Esoil*/*Ep* observed with surface soil moisture. *Esoil*/*Ep* increased almost linearly with ground surface moisture when the volumetric water content was less than 30%, but did not increase with moisture content beyond that level. When soil moisture was less than the critical value of 30%, soil evaporation was constrained by the deficiency of available water. *Kondo et al.* [1990] noted a similar critical value, reporting that the evaporation efficiency for a loam soil became 1.0 when soil moisture reached 28%. Similar relationships have been reported for the Tibetan Plateau and for Siberian tundra [*Zhang et al.*, 2003a, 2003b].

[47] Transpiration rates are determined by two parameters: leaf conductance and leaf-to-air specific deficit (*D*). Leaf conductance is a function of temperature [*Sellers et al.*, 1986; *Noilhan and Planton*, 1989; *Shuttleworth*, 1989; *Jones*, 1992]. It is impossible to present leaf conductance in this study as no CO_2 concentration data were collected. However, the right panel of Figure 12 shows the ratio of *Etrans*/*D***Pa* (*D* and *Pa* are defined in the caption of Figure 12), which directly implies a leaf conductance value, plotted in units of mms^{-1} against air temperature. The plots show that *Trans* increased as temperatures rose. When temperatures were warm, higher leaf conductance allowed water uptake if soil moisture was low, but higher than wilting point (2.8–4.1% in the root zone). Lower temperatures, lower *D*, and higher humidity accompany precipitation events, so *Trans* decreased as *Esoil* approached *E* (Figure 11).

3.7. Seasonality of Heat and Water Budget at Study Ground Surface

[48] Water conditions and atmospheric heat are both potential stressors for grass growth. However, grass cover affects heat fluxes through parameters including albedo, roughness and surface moisture. Therefore heat fluxes between the atmosphere and the ground surface are affected by grass activity, which changes in different growth periods. Heat budget components that were averaged according the grass growth period are shown in Table 2 to quantify the seasonality of heat budget. Radiative energy fluxes (*Qn*) sharply increased during pregrowth, and decreased in senescence. The ratio of atmosphere temperature stress degree days (SDD) to grass shows stable negative values in senescence. SDD was positive during early and peak growth in drier years (2002 and 2004) but negative in the wetter year (2003). Ground heat flux was positive (heat conducted to the deep soil) from pregrowth to peak growth and was

Table 2. Fluxes Averaged Over Growth Periods Including Net Radiation *Qn*, Ground Heat Flux *Qg*, Sensible Heat *Qh*, Latent Heat *Qe*, and Values of Air Temperature Stress Degree Days SDD

		Ground Surface Conditions		Mean Value of Heat Budget Components							
Period	Growth Period	Coverage of Grass, %	Biomass of Grass, gm^{-2}	Albedo, %	*Qn*, Wm^{-2}	*Qh*, Wm^{-2}	*Qe*, Wm^{-2}	*Qg*, Wm^{-2}	*Qe*/*Qn*, %	*Qh*/*Qe*	Mean SDD
1 July to 31 Aug. 2002	peak growth	35–45	45.2–53.6	18	110.8	79.4	18.5	3.8	16.7	4.3	0.39
1 Sept. to 2 Oct. 2002	senescence	no data	no data	20	69.5	61.7	8.0	−0.2	11.5	7.7	−1.09
3 Oct. 2002 to 31 March 2003	postsenescence	snow/frozen	snow/frozen	65	0.1	2.4	1.1	−2.1			
1–30 April 2003	pregrowth	bare ground	bare ground	17	115.2	85.8	26.1	3.3	22.7	3.3	
1 May to 30 June 2003	early growth	0–48	0.2–24.4	17	128.5	82.9	39.6	5.9	30.9	2.1	−0.13
1 July to 31 Aug. 2003	peak growth	52–57	49.4–114.4	16	139.4	81.9	55.2	3.9	39.6	1.5	−0.77
1 Sept. to 7 Oct. 2003	senescence	55–0	86.0–0	18	75.9	46.8	31.0	−1.9	40.8	1.5	−1.10
8 Oct. 2003 to 26 March 2004	postsenescence	snow/frozen	snow/frozen	62	1.7	2.2	4.3	−7.0			
27 March to 30 April 2004	pregrowth	bare ground	bare ground	21	105.5	87.6	12.8	5.7	12. 1	6.9	
1 May to 30 June 2004	early growth	0–29	12.1–36.4	19	131.2	101.1	18.2	8.8	13.8	5.6	0.22
Mean				27.2	87.8	63. 2	21.5	2.0	23.5	4.1	−0.4

Table 3. Integrated Ground Surface Water Budget Over Growth Periods at Study Site[a]

Period	Growth Period	Surface Soil Moisture, %	Air Temperature, deg	Mean SWS	*Pr*, mm	*E*, mm	*Ep*, mm	*E*/*Ep*, %	*Esoil*, mm	*Esoil*/*E*, %	*Etrans*, mm	*Etrans*/*E*, %
1 July to 31 Aug. 2002	peak growth	5.9	18.3	0.39	27.8	40.4	229.0	17.6	23.9	59.1	16.5	40.9
1 Sept. to 2 Oct. 2002	senescence	4.7	7.1	0.12	15.1	8.5	68.3	12.4	6.2	72.7	2.3	27.3
3 Oct. 2002 to 31 March 2003	postsenescence		−19.5		23.1	7.5						
1–30 April 2003	pre growth	20.4	1.5		2.8	14.6	67.9	21.5	14.6	100.0	0.0	0.0
1 May to 30 June 2003	early growth	17.4	11.2	1.55	70.4	52.4	267.1	19.6	45.4	86.7	7.0	13.3
1 July to 31 Aug. 2003	peak growth	14.8	14.3	1.34	81.1	87.0	328.0	26.5	75.3	86.6	11.7	13.4
1 Sept. to 7 Oct. 2003	senescence	14.4	5.8	1.36	4.7	23.6	89.2	26.5	19.1	81.0	4.5	19.0
8 Oct. 2003 to 26 March 2004	postsenescence		−19.5		41.1	13.1						
27 March to 30 April 2004	pregrowth	19.2	0.3		11.1	15.3	75.4	20.4	15.3	100.0	0.0	0.0
1 May to 30 June 2004	early growth	11.1	11.8	1.03	42.3	39.1	250.0	15.7	24.1	61.5	15.1	38.5
Total/average		9.3	−4.1	0.97	319.5	301.6	1375.0	21	223.9	78	57.1	22

[a]SWS, index of soil water stress to grass; *Pr*, index of precipitation; *E*, index of evapotranspiration; *Ep*, index of potential evaporation; *Esoil*, index of soil evaporation; and *Etran*s, index of transpiration.

negative from grass senescence through postsenescence. Turbulent heat fluxes (*Qh* and *Qe*) were fairly high outside the postsenescence period. However, seasonal variation in *Qe* clearly correlated with climate. *Qe* averaged between 39.6 and 55.2 Wm^{-2} in moist early and peak growth (2003) periods, but was stable around 18 Wm^{-2} in drier periods. The proportion of radiation driving evaporation (*Qe*/*Qn*) during periods beyond the growing season (postsenescence and pregrowth) was higher in wetter years (31–41%) than in drier years (12–17%). The Bowen ratio (*Qh*/*Qe*) shows a contrasting pattern of variation. *Qe*/*Qn* averaged 23.5% for the entire observation period. The heat fluxes during the growing season (early growth to senescence) can be substantial both in absolute magnitudes and in their relative contribution to the annual energy budget.

[49] Table 3 includes components of the ground surface water budget at the study site, integrated (averaged) over growth periods. These components include an index of soil water stress to grass (SWS), precipitation (*Pr*), evapotranspiration (*E*), potential evaporation (*Ep*), soil evaporation (*Esoil*) and transpiration (*Etrans*).

[50] In the pregrowth period, when grass stomata were not open and precipitation events were scarce, *E* was equivalent to *Esoil*. Water from snowmelt penetrated the soil but was rarely related to precipitation. Pregrowth surface soil moisture was near 20% in both 2003 and 2004, even though precipitation was different; this forced *E* (*Esoil*) to be 15 mm, and resulted in *E*/*Ep* values of ~20%. Figure 8 shows that processes causing snowmelt took about ten days, but *E* during the period was about 10% of the annual total. Similar processes have been reported in other regions of the Eurasian cryosphere, such as the Tibetan Plateau [*Zhang et al.*, 2003b, 2003c].

[51] In early and peak growth periods, *E* was significantly correlated with precipitation events (section 3.4). In wetter years (2003), precipitation during early and peak growth totaled 70.4 and 81.1 mm. *E* was 52.4 and 87.0 mm, so potential evaporation during these periods was 19.6 and 26.5%, respectively. For drier early growth periods, *E* was 39.1 mm with 42.3 mm precipitation (2004), so *Ep* was 15.7%. Similarly, for drier peak growth periods, *E* was 40.4 mm with 27.8 mm precipitation (2002), and *Ep* was 17.6%.

[52] Table 3 clearly shows the effects of precipitation (soil moisture) on the relative importance of *Esoil* and *Etrans* for *E*. In the wetter growing period (early growth to senescence) of 2003, precipitation of 156.2 mm coupled with a mean surface soil moisture of 15.5% resulted in an *Esoil* of 139.8 mm, or 84% of *E*. At this time, *Etrans* was therefore just 16% of *E*. For drier early growth periods, *Esoil* was just 24.1 mm with 42.3 mm precipitation (2004), and was 61.5% of *E*. As a consequence *Etrans* was 38.5% of *E*. For drier peak growth and senescence periods (2002), *Esoil* was 30.1 mm with 42.9 mm precipitation, and was 61.6% of *E*; *Etrans* was 38.5% of *E*. Section 3.6 describes the correlation between *Etrans* and climate. The correlation may increase during drier periods because of higher temperatures, and decrease in wetter periods because of lower temperatures and lower leaf-to-air specific deficits. Table 3 shows that the air temperature was noticeably higher in the drier growing period. Mean temperatures in drier early growth (2004), and in drier peak growth and drier senescence (2002) periods were higher than mean temperatures in wetter periods (2003). Over semiarid grassland, grass plays an important role in controlling evaporation processes in relatively drier years.

4. Summary and Concluding Remarks

[53] The study region was characterized by a dry atmosphere, dry soil, and low grass production. In accordance with phenological processes and PAR albedo variation, grass growth periods at the site could be divided into four stages by the temporal change in PAR albedo and biomass: pregrowth, early growth, peak growth and senescence. The season after the ground surface became covered by stable snow cover was defined as the postsenescence. The grass growing period included early growth, peak growth and senescence periods of roughly 2 months, 2 months and 1 month in length, respectively. Cold temperatures allowed postsenescence to persist for half a year, a characteristic similar to other cryospheres. The length of every growing period is different from the results of warmer regions, such as north-central Oklahoma of the United States [*Burba and Verma*, 2001]; the growing period at the study site is characterized by shorter peak growth and senescence, but a quite long postsenescence period. Although the observation site was underlain by warm permafrost, a thawing front quickly penetrated to 3 m. This meant that thaw-freeze dynamics did not significantly affect land surface hydrologic processes during the grass growing season.

[54] The index of air temperature stress degree day (SDD) and soil water stress (SWS) index have been evaluated at

the study site to investigate the response of grass growing to atmospheric and soil water forcing. SDD was small and prevailingly negative. Variations in the soil water stress index tracked precipitation fluctuations. The index was stable at 1.4 in wetter growing periods but was smaller in drier periods. Variability of the two indexes may imply that atmospheric heat stress for the growing grass was weak compared to soil water stress for a semiarid region. The above conclusion is supported by irrigation experimental observation as well; clear differences of biomass were observed between watered ground and unwatered ground after irrigation commenced. The results of this work show a significant difference of biomass between drier and moister years, which correlated well with precipitation. A similar conclusion has been deduced in the region south [*Ni*, 2003] and west [*Miyazaki et al.*, 2004] of the study site. The former revealed a positive relationship between a grass-growing index and precipitation distribution in northeast China and southeast Mongolia; the latter suggest that the precipitation before July had the most influence on grass growth in central Mongolia.

[55] At such a semiarid ground surface, water supply has been clarified to be a dominant factor driving heat/water fluxes in the soil-vegetation-atmosphere mechanism. The evidence can be read from the temporal decline processes of grass of evapotranspiration (E) and ratio of E to potential evaporation, which relates to the precipitation events or snowmelt. Even if net radiation flux were steady and high through the early and peak growth periods, turbulent heat flux was affected by surface moisture. Latent heat flux and its relative importance to net radiation were several times higher during wetter growing periods compared to drier periods.

[56] Parameterization of soil evaporation (*Esoil*) using soil surface moisture provides a useful tool to partition E into transpiration (*Etrans*) and *Esoil*. Microlysimeter observations of calculated soil evaporation and evapotranspiration demonstrated that partitioning was a reasonable approach in the study region. Evapotranspiration shows different seasonality relating to precipitation. During the wetter growing period of 2003, evapotranspiration was 163.0 mm, 57% of the 2-year total. Transpiration values had different relationships with precipitation or ground surface moisture values. *Etrans*/E was 14% in the wetter grass-growing period (2003) but was 38.5% in the drier early growth period (2004) and was 40.9% in the drier peak growth period (2002). These proportions were determined by high leaf conductance in drier periods and lower leaf-to-air specific deficits in wetter periods. In the observation period, which spanned two cycles of pregrowth to post-senescence, evapotranspiration totaled 286.9 mm, and precipitation totaled 255.3 mm. The transpiration partition was 22%. Seasonal variability suggested that 88% of E and 94% of the precipitation occurred during the grass growth period (early growth to senescence). Even though the growing period is quite short in peripheral regions of the cryosphere, water fluxes between the atmosphere and the ground surface during the growing period contribute significantly to the annual water cycle.

[57] Over the entire study period, precipitation totaled 319.5 mm, and E was 301.6 mm. Precipitation was nearly balanced by E during the study period, which shows a similar regime to the results of *Ma et al.* [2003] and *Miyazaki et al.* [2004], and also the classical estimated value of water budget in study region [*Tuvendendorzh and Myagmarzhav*, 1985]. Potential evapotranspiration was estimated to be values of 5 times that of precipitation. Transpiration was enhanced in drier summer by higher temperature. In summary, the higher evaporative ability of atmosphere, higher water transportability of grass coupling to climatic warming, and pulsing lower water capacity of the ground surface layer (Figure 2) are anticipated to be the cause of desertification-related degradation of the ecosystem, which is occurring at a tremendous rate in the study region [*Gunin et al.*, 1999].

[58] **Acknowledgment.** Grateful thanks are extended to D. Azzaya, G. Davaa, and D. Uyunbaatar for their help and cooperation with our field work in Mongolia.

References

Allen, S. J. (1990), Measurement and estimation of evaporation from soil sparse barley vegetations in northern Syria, *Agric. For. Meteorol.*, *49*, 291–309.

Beaubien, E. G., and H. J. Freeland (2000), Spring phenology trends in Alberta, Canada: Links to ocean temperature, *Int. J. Biometeorol.*, *44*, 53–59.

Bereneva, I. A. (1992), Peculiarities of studies and methods of assessment of climatic resources of complex ecosystems of Mongolia (in Russian), in *Ecology and Nature Management in Mongolia*, edited by N. I. Dorofeyuk, pp. 25–32, GUGK, Moscow.

Brutsaert, W. (1982), *Evaporation Into the Atmosphere*, 216 pp., Springer, New York.

Burba, G. G., and S. B. Verma (2001), Prairie growth, PAR albedo and seasonal distribution of energy fluxes, *Agric. For. Meteorol.*, *107*, 227–240.

Burba, G. G., S. B. Verma, and J. Kim (1999), Surface energy fluxes of *Phragmites australis* in a prairie wetland, *Agric. For. Meteorol.*, *94*, 31–51.

Chapin, F. S. (2000), Role of terrestrial ecology in arctic hydrologic systems, in *Meeting White Papers of NSF-ARCSS Workshop on Arctic System Hydrology*, compiled by C. Vörösmarty and L. Hinzman, pp. 12–13, Natl. Cent. for Ecol. Anal. and Synthesis, Santa Barbara, Calif.

Chmielewski, F.-M., and T. Rotzer (2001), Response of tree phenology to climate change across Europe, *Agric. For. Meteorol.*, *180*, 101–112.

Dickinson, R. E. (1987), Evaporation in global climate models, *Adv. Space Res.*, *7*(11), 17–26.

Gunin, P. D., A. V. Elizabeth, I. D. Nadezhda, P. E. Tarasov, and C. C. Black (Eds.) (1999), *Vegetation Dynamics of Mongolia*, pp. 9–15, Springer, New York.

Hutjes, R. W. A., et al. (1998), Biospheric aspects of the hydrological cycle, *J. Hydrol.*, *212–213*, 1–21.

Idso, S. B. (1982), Non-water-stress baselines: A key to measuring and interpreting plant water stress, *Agric. Meteorol.*, *27*, 59–70.

Idso, S. B., R. D. Jackson, and R. J. Reginato (1977), Remote sensing of vegetation yields, *Science*, *196*, 19.

Ishikawa, M., N. Sharkhuu, Y. Zhang, T. Kadota, and T. Ohata (2005), Ground thermal and moisture conditions at the southern boundary of discontinuous permafrost, Mongolia, *Permafrost Periglacial Processes*, *16*, 209–216.

Jackson, R. D. (1982), Grass temperature and vegetation water stress, in *Advances in Irrigation*, edited by D. Hillel, vol. 1, pp. 43–85, Elsevier, New York.

Jackson, R. D., R. J. Reginato, and S. B. Idso (1977), Wheat grass temperature: A practical tool for evaluating water requirements, *Water Resour. Res.*, *13*, 651–656.

Jones, H. G. (1992), *Plants and Microclimate*, 2nd ed., pp. 156–157, Cambridge Univ. Press, New York.

Kim, J., and S. B. Verma (1996), Surface exchange of water vapor between an open sphagnum fen and the atmosphere, *Boundary Layer Meteorol.*, *79*, 243–264.

Kirkham, M. B., D. E. Johnson, E. Kanemasu, and L. R. Stone (1983), Grass temperature and growth of differentially irrigated alfalfa, *Agric. For. Meteorol.*, *29*, 235–248.

Kondo, J., N. Saigusa, and T. Sato (1990), A parameterization of evaporation from bare soil surfaces, *J. Appl. Meteorol.*, *29*, 385–389.

Lascano, R. J., R. L. Baumhardt, S. K. Hicks, and J. L. Heilman (1994), Soil and plant water evaporation from strip-tilled cotton: Measurement and simulation, *Agron. J.*, *86*, 987–994.

Lingakumar, K., and G. Kulandaivelu (1998), Differential responses of growth and photosynthesis, in *Cyamopsis tetragonoloba* L. grown under ultraviolet-B and supplemental long-wavelength radiations, *Photosynthetica*, *35*, 335–343.

Lucht, W., et al. (2002), Climatic control of the high-latitude vegetation greening trend and Pinatubo effect, *Science*, *296*, 1687–1689.

Ma, X., T. Yasunari, T. Ohata, L. Natsagdorj, G. Davaa, and D. Oyunbaatar (2003), Hydrological regime analysis of the Selenge River Basin, Mongolia, *Hydrol. Processes*, *17*, 2929–2945.

Miyazaki, S., T. Yasunari, T. Miyamoto, I. Kaihotsu, G. Davaa, D. Oyunbaatar, L. Natsagdorj, and T. Oki (2004), Agrometeorological conditions of grassland vegetation in central Mongolia and their impact for leaf area growth, *J. Geophys. Res.*, *109*, D22106, doi:10.1029/2004JD005179.

Myneni, R. B., et al. (1997), Increased plant growth in the northern high altitudes from 1981 to 1991, *Nature*, *386*, 698–702.

Nemani, R. R., C. D. Keeling, H. Hashimoto, W. M. Jolly, S. C. Piper, C. J. Tucker, R. B. Myuneni, and S. W. Running (2003), Climate-driven increase in global terrestrial net primary production from 1982 to 1999, *Science*, *300*, 1560–1563.

Ni, J. (2003), Plant functional types and climate along a precipitation gradient in temperate grasslands, north-east China and south-east Mongolia, *J. Arid Environ.*, *53*, 501–516.

Nogina, N. A. (Ed.) (1978), *Soil Survey of the Main Natural Zones of Mongolia* (in Russian), 275 pp., Nauka, Moscow.

Nogina, N. A. (1989), Specific features of soils and soil formation processes in the central Asian facies (taiga, steppe, desert) (in Russian), *Soil Sci.*, *9*, 5–14.

Noilhan, J., and S. Planton (1989), A simple parameterization of land surface processes for meteorological model, *Mon. Weather Rev.*, *117*, 536–549.

Oke, T. (1987), *Boundary Layer Climates*, 2nd ed., pp. 382–384, Methuen, New York.

Pearcy, R. W., D. Bijorkman, A. T. Harrison, and H. A. Moorey (1971), Photosynthetic performance of two desert species with C-4 photosynthesis in Death Valley, California, *Year Book Carnegie Inst. Washington*, *70*, 540.

Sakai, R. K., D. R. Fitzjarrald, and K. E. Moore (1997), Detecting leaf area and surface resistance during transition seasons, *Agric. For. Meteorol.*, *84*, 273–284.

Schwartz, M. D. (1999), Advancing to full bloom: Planning phenological research for the 21st century, *Int. J. Biometeorol.*, *42*, 113–118.

Sellers, P. J., Y. Mintz, Y. C. Sud, and A. Dalcher (1986), A Simple Biosphere Model (SiB) for use within general circulation models, *J. Atmos. Sci.*, *43*(6), 505–531.

Sharkhuu, N. (2001), Dynamics of permafrost in Mongolia, Tohoku, *Geophys. J.*, *36*(2), 91–99.

Shaver, R., et al. (2000), Global warming and terrestrial ecosystems: A conceptual framework for analysis, *BioScience*, *50*(10), 871–882.

Shuttleworth, W. J. (1989), Micrometeorology of temperate and tropical forest, *Philos. Trans. R. Soc. London, Ser. B*, *324*, 299–334.

Sivakumar, M. V. K. (1986), Grass-air temperature differentials, water use and yield of chickpea in a semi-arid environment, *Irrig. Sci.*, *7*, 149–158.

Tsegmid, S., , and V. V. Vorobiev (Eds.) (1990), *The National Atlas: Mongolian People's Republic* (in Russian), 144 pp., GUGK, Moscow.

Tuvendendorzh, D., and B. Myagmarzhav (Eds.) (1985), *The Atlas of the Climate and Ground Water Resources in Mongolian People's Republic*, 73 pp., Inst. of Meteorol. and Hydrol., Ulan Bator, Mongolia.

Vörösmarty, C. J., L. D. Hinzman, B. J. Peterson, D. H. Bromwich, L. C. Hamilton, J. Morison, V. E. Romanovsky, M. Sturm, and R. S. Webb (2001), The hydrologic cycle and its role in the Arctic and global environmental change: A rationale and strategy for synthesis study, 84 pp., Arct. Res. Consortium, Fairbanks, Alaska.

Walker, G. K., and J. L. Hatfield (1979), Test of stress-degree-day concept using multiple planting dates of red kidney beans, *Agron. J.*, *71*, 967.

Yokoyama, K., H. Ohno, Y. Kominami, S. Inoue, and T. Kawakata (2003), Performance of Japanese precipitation gauges in winter, *J. Jpn. Soc. Snow Ice*, *65*, 303–316.

Zhang, Y., T. Ohata, E. Kang, and T. Yao (2003a), Observation and estimation of evaporation from the ground surface of the cryosphere in eastern Asia, *Hydrol. Processes*, *17*, 1135–1147.

Zhang, Y., T. Ohata, and T. Kadota (2003b), Land-surface hydrological processes in the permafrost region of the eastern Tibetan Plateau, *J. Hydrol.*, *283*, 41–56.

Zhang, Y., T. Kadota, and T. Ohata (2003c), Land-surface hydrological processes in discontinuous permafrost region of the western Tibetan Plateau, paper presented at 8th International Conference on Permafrost, Int. Permafrost Assoc., Zurich, 21–25 July.

Zhang, Y., T. Ohata, D. Yang, and G. Davaa (2004), Bias correction of daily precipitation measurements for Mongolia, *Hydrol. Processes*, *18*, 2991–3005.

T. Kadota, T. Ohata, and Y. Zhang, Institute of Observational Research for Global Change, IORGC/JAMSTEC, 2-15 Natsushima-cho, Yokosuka 237-0061, Japan. (yszhang@jamstec.go.jp)

E. Munkhtsetseg, Arid Land Research Center, Tottori University, Tottori 680-0001, Japan.